

This article was downloaded by:

On: 25 January 2011

Access details: *Access Details: Free Access*

Publisher *Taylor & Francis*

Informa Ltd Registered in England and Wales Registered Number: 1072954 Registered office: Mortimer House, 37-41 Mortimer Street, London W1T 3JH, UK



## Liquid Crystals

Publication details, including instructions for authors and subscription information:

<http://www.informaworld.com/smpp/title~content=t713926090>

### High birefringence phenyl tolane positive compounds for dual frequency liquid crystals

Jie Sun<sup>a</sup>; Haiqing Xianyu<sup>a</sup>; Sebastian Gauza<sup>a</sup>; Shin-Tson Wu<sup>a</sup>

<sup>a</sup> College of Optics and Photonics, University of Central Florida, Orlando, FL, USA

Online publication date: 14 December 2009

**To cite this Article** Sun, Jie , Xianyu, Haiqing , Gauza, Sebastian and Wu, Shin-Tson(2009) 'High birefringence phenyl tolane positive compounds for dual frequency liquid crystals', *Liquid Crystals*, 36: 12, 1401 – 1408

**To link to this Article:** DOI: 10.1080/02678290903242968

**URL:** <http://dx.doi.org/10.1080/02678290903242968>

PLEASE SCROLL DOWN FOR ARTICLE

Full terms and conditions of use: <http://www.informaworld.com/terms-and-conditions-of-access.pdf>

This article may be used for research, teaching and private study purposes. Any substantial or systematic reproduction, re-distribution, re-selling, loan or sub-licensing, systematic supply or distribution in any form to anyone is expressly forbidden.

The publisher does not give any warranty express or implied or make any representation that the contents will be complete or accurate or up to date. The accuracy of any instructions, formulae and drug doses should be independently verified with primary sources. The publisher shall not be liable for any loss, actions, claims, proceedings, demand or costs or damages whatsoever or howsoever caused arising directly or indirectly in connection with or arising out of the use of this material.

## High birefringence phenyl tolane positive compounds for dual frequency liquid crystals

Jie Sun, Haiqing Xianyu\*, Sebastian Gauza and Shin-Tson Wu

College of Optics and Photonics, University of Central Florida, Orlando, FL 32816, USA

(Received 21 July 2009; final form 7 August 2009)

Dual frequency liquid crystals (DFLCs) provide a possibility to achieve sub-millisecond rise and decay times and are useful for various electro-optical devices. In most of DFLC mixtures, ester compounds are utilised in order to obtain a low crossover frequency. However, the ester linking group does not provide  $\pi$  electron conjugation so that the DFLC mixtures usually exhibit a limited birefringence ( $\Delta n < 0.3$  at  $\lambda = 633$  nm). For phase modulation a lower birefringence demands a thicker cell gap which, in turn, increases the response time and operating voltage. This problem becomes more severe as the wavelength increases. In this paper, we introduce a series of isothiocyanato phenyl tolane positive compounds with high birefringence and moderate dielectric relaxation frequency. The dielectric and electro-optical properties of these compounds are investigated. We also formulated a DFLC mixture using these new positive compounds which exhibits  $\Delta n = 0.39$  at  $\lambda = 633$  nm and  $0.33$  at  $\lambda = 1550$  nm.

**Keywords:** high birefringence; dual frequency liquid crystals

### 1. Introduction

In addition to their widespread applications in information displays (1), liquid crystals (LCs) are also useful for electro-optical devices such as spatial light modulators (2, 3), variable optical attenuators (4, 5), light shutters (6), tunable filters (7) and adaptive optics (8). The continuous demand for a faster response time in these devices has fostered the development of new LC materials and driving methods. Nematic LCs with high birefringence ( $\Delta n$ ), low visco-elastic coefficient, and large dielectric anisotropy ( $\Delta\epsilon$ ) have been developed to achieve fast response. High  $\Delta n$  LCs enable a thinner cell gap to achieve the same phase change, and thereby efficiently reduce the response time (9–11). This is especially important for devices operating in the infrared (IR) region (12, 13), where a thicker cell gap is required in order to compensate for the longer wavelength. Driving schemes such as overdrive and undershoot have been introduced to decrease the response time (14, 15). However, only the turn-on process can be accelerated by the applied overdrive voltage. Efforts to reduce decay time are limited by the LC properties and alignment conditions when using an ordinary nematic LC. Dual frequency liquid crystals (DFLCs) (16, 17) offer a possibility to break this barrier by an electrically-assisted LC relaxation process.

DFLC mixtures usually comprise two kinds of materials (18). First, there are compounds that exhibit a positive  $\Delta\epsilon$  when addressed by a low frequency (in the kilohertz range) electric field and whose dielectric anisotropy decreases as the driving frequency increases. These compounds (referred to as positive compounds) provide the positive  $\Delta\epsilon$  at low

frequencies and the frequency dependence of dielectric anisotropy. Second, there are compounds that exhibit a constant but negative  $\Delta\epsilon$  when the driving frequency above  $\sim 1$  MHz. These negative compounds provide the large negative  $\Delta\epsilon$  at high frequencies. Similar to ordinary LCs, high  $\Delta n$  DFCL materials are equally favoured from fast response time and low operating voltage viewpoints. Highly conjugated negative compounds with a relatively high birefringence ( $\Delta n > 0.3$ ) have been adopted in recently developed DFCL mixtures (19–22). However, those negative compounds whose  $\Delta n$  is larger than 0.35 often exhibit a high melting temperature or relatively small dielectric anisotropy, setting a limit on their possible adoption ratio in DFCL mixtures (23).

Since the discovery of the DFCL effect in the 1970s (16), almost every low crossover frequency DFCL mixture contains at least one ester group in the positive compounds (24–26). The ester group serves two important purposes: 1) it enhances the positive dielectric anisotropy at low frequencies, and 2) it provides a slightly negative  $\Delta\epsilon$  at high frequencies. However, the ester group does not provide conjugated  $\pi$  electrons. The  $\pi$  electron conjugation length, and thereby the birefringence of the ester compounds, are limited, usually  $\Delta n < 0.3$  at  $\lambda = 633$  nm. High birefringence positive compounds play an important role for enhancing the  $\Delta n$  of DFCL mixtures.

In this paper, we introduce a new series of positive compounds with a highly conjugated  $\pi$ -electron core structure for DFCL mixtures. The dielectric relaxation and electro-optical properties of these compounds were characterised and compared with ester

\*Corresponding author. Email: hxianyu@creol.ucf.edu

compounds having a similar structure. A high  $\Delta n$  DF LC mixture using these compounds was formulated and its physical properties evaluated.

## 2. Compound structures

### 2.1 Positive $\Delta\epsilon$ compounds

The most efficient way to increase birefringence is to enhance the electron conjugation length (27). This can

be achieved by either elongating the conjugated core structure, e.g. terphenyl, tolane, and bistolane, or attaching an electron acceptor polar group, e.g. cyano (CN) and isothiocyanato (NCS) (28–34). Recently, some NCS phenyl-tolane compounds with  $\Delta n \sim 0.5$  at  $\lambda = 633$  nm and  $T = 23^\circ\text{C}$  were investigated (35, 36). One series of phenyl tolane compounds (#1–3 in Table 1) attracted our attention for DF LC applications.

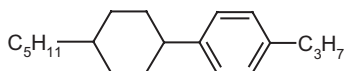
Table 1. Molecular structures and phase transition temperatures of the positive compounds under study. Here, Cr, N, S, and I stand for crystalline, nematic, smectic, and isotropic phase.  $\Delta H$  (in unit of kcal/mol) is the heat fusion enthalpy for the Cr–N transition.

No.	Notation	Molecular structures	Phase transition temperatures ( $^\circ\text{C}$ )	$\Delta H$
1	PP(23F)TP(3F)-2NCS		Cr 73.7 N 223.3 I	5.45
2	PP(23F)TP(3F)-3NCS		Cr 82.2 S 89.2 N 240.5 I	5.81
3	PP(23F)TP(3F)-5NCS		Cr 53.5 S 135.0 N 218.0 I	3.36
4	CPEP(3F)-3CN		Cr 100.3 N 201.1 I	4.68
5	CPEP(3F)-5CN		Cr 92.3 N 194.4 I	5.21
6	PPEP(3F)-3CN		Cr 95.6 N 201.0 I	5.51
7	PPEP(3F)-5CN		Cr 79.2 N 190.0 I	6.85
8	CPEP(3F)-3NCS		Cr 108.2 N 226.3 I	5.39
9	CPEP(3F)-5NCS		Cr 85.6 N 218.6 I	4.98
10	PPEP(3F)-3NCS		Cr 91.9 S 153.5 N 234.7 I	4.03
11	PPEP(3F)-5NCS		Cr 87.5 S 175.0 N 220.2 I	3.18

In this structure, the middle phenyl ring has two fluoro substitutions in the second and third positions while the last ring has a single fluoro substitution at the third position which is adjacent to the NCS terminal group. The lateral difluoro group on the middle ring provides an effective dipole moment perpendicular to the principal molecular axis, which will contribute to a negative  $\Delta\epsilon$  at high frequencies. On the other hand, the total dipole moment of the single fluoro and the NCS terminal group is approximately parallel to the principal molecular axis, contributing to positive  $\Delta\epsilon$  at low frequencies. The long rigid core structure leads to a relatively low dielectric relaxation frequency. Such a unique structure allows these compounds to replace the ester-based positive compounds in DF LC mixtures. Since NCS phenyl-tolane molecules are linearly conjugated, they exhibit a significantly higher birefringence than the comparative esters.

## 2.2 Positive $\Delta\epsilon$ mixtures

Table 1 lists the positive compounds we studied and their phase transition temperatures and heat fusion enthalpies. Ideally, we should evaluate the physical properties of each positive compound individually. However, both phenyl-tolane and ester compounds have a relatively high melting temperature and some exhibit smectic phase. Thus, we measured their physical properties in mixtures. In the first experiment, we formulated three positive  $\Delta\epsilon$  mixtures using the similar molecular structures listed in Table 1; say P1 mixture contains compounds #1–3 (NCS phenyl-tolane), P2 contains #4–7 (three ring single ester CN compounds), and P3 contains #8–11 (three ring single ester NCS compounds). In P2 and P3 mixtures, some cyclohexane compounds (#4–5 and #8–9) are included in order to improve the mesomorphic properties. However, the melting points of these mixtures are still far above room temperature and, moreover, P1 and P3 exhibit smectic phases at room temperature. Thus, we added the following non-polar diluter (CP-53, structure in Scheme 1) to each mixture in order to lower the melting point and suppress the smectic phase:



Scheme 1. Chemical structure of nonpolar diluter CP-53.

CP-53 has a melting point at  $-5.6^\circ\text{C}$ , thus it is an isotropic liquid at room temperature ( $T \sim 23^\circ\text{C}$ ). Detailed compositions are summarised as follows: Mixture-A consists of 69 wt% P1 and 31 wt% CP-53; Mixture-B 69 wt% P2 and 31 wt% CP-53; and Mixture-C 69 wt% P3 and 31 wt% CP-53. In all three

mixtures, we keep the concentration of CP-53 the same in order to readily compare the performance of P1, P2 and P3. Mixtures A, B, and C all exhibit nematic phase at room temperature; their clearing temperatures are  $\sim 129^\circ\text{C}$ ,  $\sim 122^\circ\text{C}$ , and  $\sim 136^\circ\text{C}$ , respectively.

## 3. Experimental

### 3.1 Dielectric relaxation measurement

Two cells with homogeneous alignment and homeotropic alignment, respectively, are used in this study. Cell gap was controlled at  $d \sim 8 \mu\text{m}$ . By comparing the capacitance of the cell before and after filling the LC mixture, frequency dependent dielectric permittivity along the principal molecular axis ( $\epsilon_{\parallel}$ ) of the material can be obtained (37). Similarly, we measured the dielectric permittivity perpendicular to the principal molecular axis ( $\epsilon_{\perp}$ ) using the homeotropic cell. Once  $\epsilon_{\parallel}$  and  $\epsilon_{\perp}$  are obtained, we can calculate  $\Delta\epsilon$  through  $\epsilon_{\parallel} - \epsilon_{\perp}$ . We also measured the frequency-dependent dielectric constant of CP-53. Its value ( $2.22 \pm 0.06$ ) is independent of frequency in the 100 Hz to 5 MHz range.

### 3.2 Electro-optical measurement

Homogeneous cells with cell gap  $d \sim 5 \mu\text{m}$  and pretilt angle  $\theta \sim 2\text{--}3^\circ$  were employed in this experiment. A linearly polarised He-Ne laser ( $\lambda = 633 \text{ nm}$ ) was utilised as the light source. After filling a cell with the LC mixture, we placed it between two crossed polarisers and measured its phase retardation  $\delta$ , which is expressed as (38):

$$\delta = 2\pi d \Delta n / \lambda. \quad (1)$$

Once  $\delta$  is obtained, birefringence of the mixture can be calculated from Equation (1). The visco-elastic coefficient of the materials is obtained by measuring the free relaxation time of the sample cell (37). For IR measurements, the light source employed is a laser diode with  $\lambda = 1.55 \mu\text{m}$ .

## 4. Results of positive $\Delta\epsilon$ mixtures

### 4.1 Dielectric properties

Low relaxation frequency is a prerequisite for positive compounds for DF LCs. Figures 1(a), 1(b), and 1(c) depict the frequency-dependent dielectric anisotropy of Mixture-A, Mixture-B, and Mixture-C, respectively, at a series of temperatures. The experimental results fit well with the following Debye equation (23):

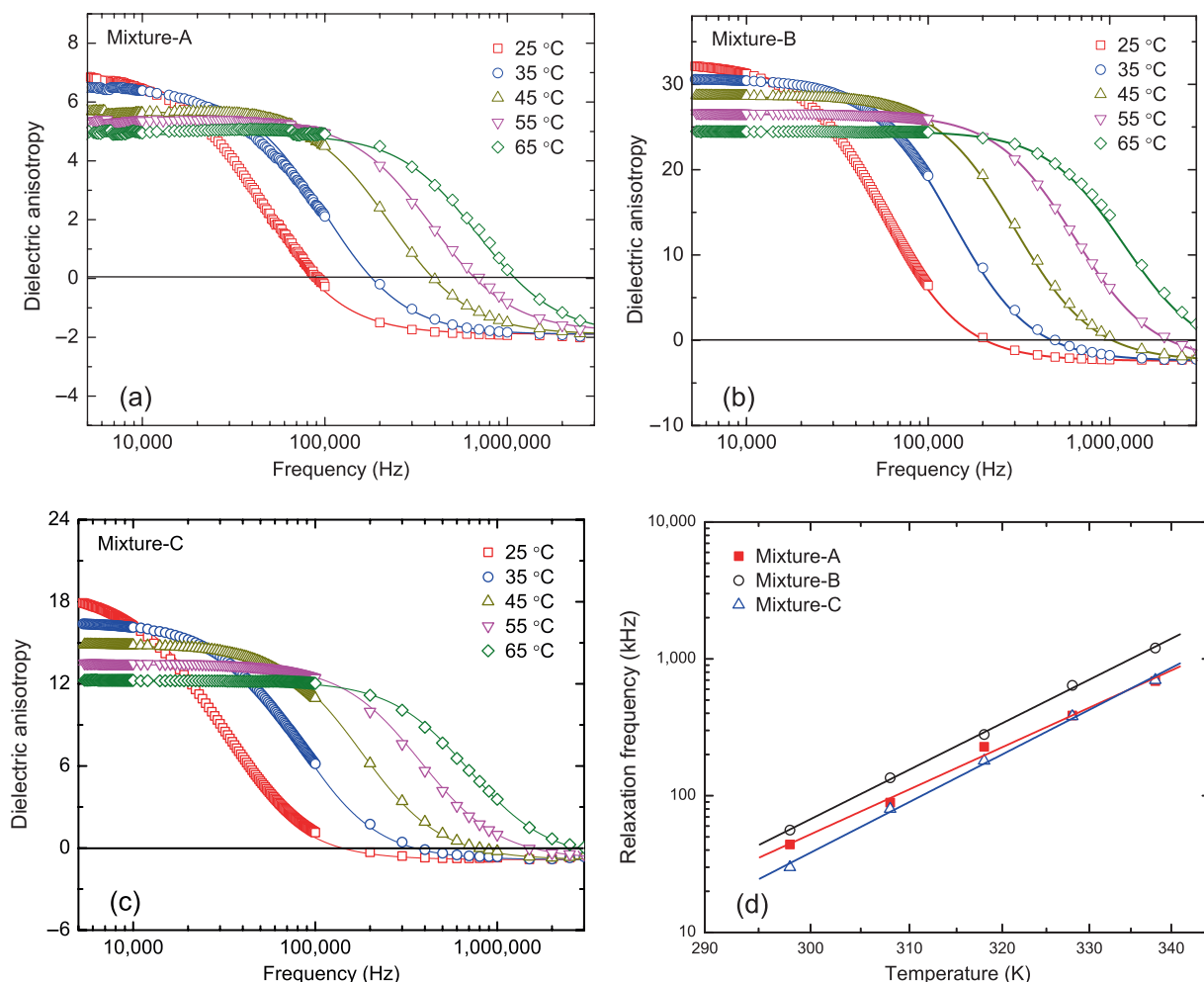


Figure 1. Frequency-dependent dielectric anisotropy of (a) Mixture-A, (b) Mixture-B, and (c) Mixture-C under different temperatures, while (d) shows the temperature-dependent relaxation frequency of the three mixtures. Symbols denote experimental results while solid lines correspond to fitting results.

$$\Delta\varepsilon(f) = \Delta\varepsilon(\infty) + \frac{\Delta\varepsilon(0) - \Delta\varepsilon(\infty)}{1 + (f/f_r)^2}, \quad (2)$$

where  $\Delta\varepsilon(0)$  and  $\Delta\varepsilon(\infty)$  represent the dielectric anisotropy at low frequency limit and high frequency limit, respectively,  $f$  is the driving frequency, and  $f_r$  is the relaxation frequency. The temperature-dependent  $f_r$  is plotted in Figure 1(d) for the three mixtures studied. As the temperature increases,  $f_r$  increases exponentially, which can be described by the following equation (39):

$$f_r \sim \exp(-E_I/k_B T), \quad (3)$$

where  $E_I$  is the activation energy,  $k_B$  is the Boltzmann constant, and  $T$  is the Kelvin temperature. The fitted  $\Delta\varepsilon(0)$ ,  $\Delta\varepsilon(\infty)$ ,  $f_r$  at 25 °C and activation energy ( $E_I$ ) for the three mixtures are listed in Table 2. It is noted that Mixture-A shows a comparable relaxation frequency

Table 2. Dielectric relaxation properties of Mixture-A, Mixture-B, and Mixture-C at  $T = 25^\circ\text{C}$ .

	$\Delta\varepsilon(0)$	$\Delta\varepsilon(\infty)$	$f_r$ (kHz)	$E$ (meV)
Mixture-A	7.1	-1.9	44	606.0
Mixture-B	32.5	-2.4	56	667.6
Mixture-C	18.6	-0.9	30	683.7

with respect to that of the other two mixtures. The relatively low activation energy of Mixture-A gives a smaller increment in  $f_r$  as the temperature increases. Among the three mixtures, Mixture-A exhibits the smallest  $\Delta\varepsilon(0)$ . At 25 °C, the fitted  $\Delta\varepsilon(0)$  of Mixture-A is 7.1, much smaller than that of Mixture-B (32.5) and Mixture-C (18.6). Mixture-B has the largest dielectric anisotropy because the CN terminal group has a larger dipole moment than NCS. At high frequency limit, however, Mixture-A shows a negative dielectric



anisotropy ( $\Delta\varepsilon(\infty) = -1.9$ ) slightly smaller than that of Mixture-B ( $-2.4$ ), but larger than Mixture-C ( $-0.9$ ). Since Mixture-A has the largest  $|\Delta\varepsilon(\infty)/\Delta\varepsilon(0)|$  ratio, less negative compounds are required if we use the new phenyl-tolane-based positive compounds instead of the traditional esters to formulate DF LC mixtures. A detailed discussion will follow.

## 4.2 Electro-optical properties

The birefringence and visco-elastic coefficient ( $\gamma_1/K_{11}$ ) of Mixtures A, B, and C were measured at elevated temperatures. The temperature-dependent birefringence (40, 41) and visco-elastic coefficient (42) have the following forms:

$$\Delta n = \Delta n_0(1 - T/T_c)^\beta, \quad (4)$$

$$\gamma_1/K_{11} \sim \exp(E_2/k_B T)/(1 - T/T_c)^\beta, \quad (5)$$

where  $\Delta n_0$  is the birefringence at  $T = 0$  K,  $T_c$  is the clearing temperature of the LC material,  $\beta$  is a material constant,  $K_{11}$  is the splay elastic constant,  $\gamma_1$  is the rotational viscosity,  $E_2$  is the activation energy of molecular rotation,  $k_B$  is the Boltzmann constant, and  $T$  is the Kelvin temperature. A He-Ne laser with wavelength  $\lambda = 633$  nm and homogeneous LC cells were employed in this experiment.

Figure 2(a) shows a comparison of the measured birefringence and the fitting curves for the three mixtures as a function of temperature. With increasing temperature, the birefringence decreases gradually. In accordance with our prediction, Mixture-A exhibits a significantly higher birefringence than the other two mixtures due to the longer conjugation length of phenyl tolane. Since the birefringence of the neutral diluter CP-53 is small ( $\sim 0.05$ ), we are able to extrapolate the birefringence of the phenyl tolane positive compounds, which is as high as 0.47 at 25°C. This result agrees well with that reported by Gauza *et al.* (35). Also, NCS-based compounds have a longer  $\pi$ -electron conjugation length than the corresponding CN-based compounds, so Mixture-C shows a higher birefringence than Mixture-B as expected.

Figure 2(b) shows the measured visco-elastic coefficient of Mixtures A, B, and C, in which symbols are experimental data and lines are fitting results with Equation (5). As temperature increases, the visco-elastic coefficient first decreases rapidly and then gradually saturates. At  $T = 25^\circ\text{C}$ , Mixture-A has a similar visco-elastic coefficient (10.3) to Mixture-C, which is  $\sim 3\times$  smaller than that of Mixture-B (40.2). This is because the rotational viscosity of Mixture-B is significantly increased by the dimers formed between the molecules of CN compounds.

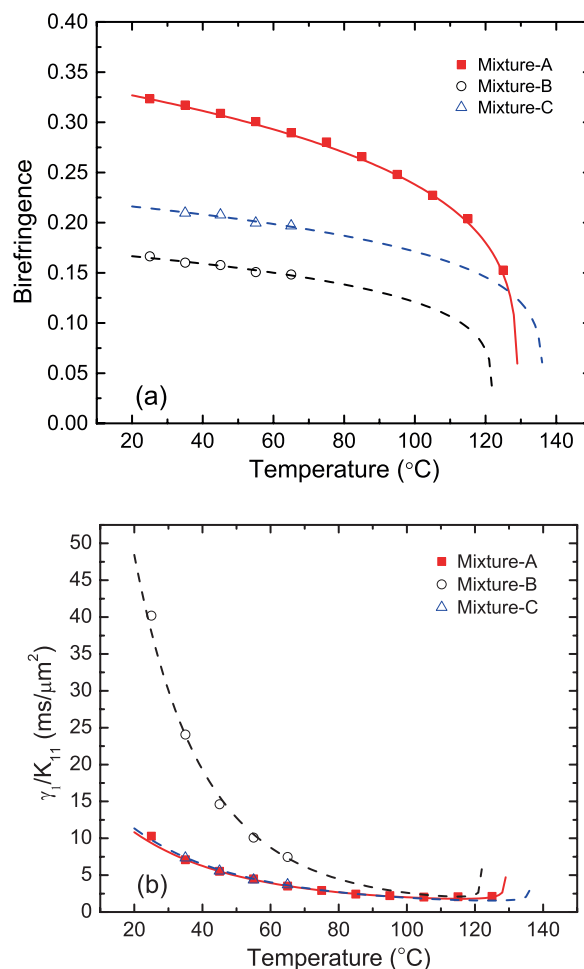
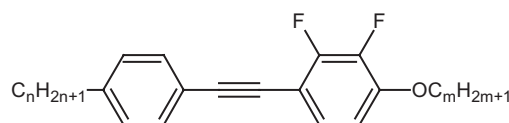


Figure 2. Experimental (symbols) and fitting (curves) results of temperature-dependent (a) birefringence and (b) visco-elastic coefficient of Mixture-A, Mixture-B and Mixture-C.

## 5. DF LC mixtures

In Section 3, above, we characterised the physical properties of three positive  $\Delta\varepsilon$  mixtures. However, the ultimate goal is to form DF LC mixtures. To obtain a low crossover frequency ( $< 10$  kHz), we normally mix a large  $\Delta\varepsilon$  mixture in a negative  $\Delta\varepsilon$  host at  $\sim 30:70$  ratio. The negative host plays a crucial role in determining the final performance of the DF LC mixture (39). Our goal is to formulate a high  $\Delta n$  DF LC mixture for IR applications, e.g. adaptive optics at  $\lambda = 1.55$   $\mu\text{m}$ . Thus, we prepared a negative  $\Delta\varepsilon$  LC host primarily consisting of following lateral difluoro-tolane homologues (Scheme 2) (20):



Scheme 2. Chemical structure of the major components of the negative dielectric anisotropy LC host.

For the convenience of discussion, we designate this negative  $\Delta\epsilon$  LC mixture as N1.

To fairly compare the performance of DFCLC mixtures is not an easy task because there are several parameters involved, such as birefringence, viscosity, dielectric anisotropy and crossover frequency. In our experiment, we set a criterion that  $\Delta\epsilon(0) \sim \Delta\epsilon(\infty)$  so that the rise and decay times of each mixture would be symmetric. We prepared three DFCLC mixtures: DFCLC-A, -B and -C. To achieve approximately equal dielectric anisotropy at low and high frequency limits, these three DFCLC mixtures contain different ratios of positive components to N1. DFCLC-A contains 60 wt% P1 and 40 wt% N1, DFCLC-B contain 20 wt% P2 and 80 wt% N1, and DFCLC-C contains 30 wt% P3 and 70 wt% N1.

### 5.1 Dielectric anisotropy

Figures 3(a) to 3(c) depict the frequency-dependent dielectric anisotropy of DFCLC-A, -B and -C, respectively, at elevated temperatures. Table 3 shows the fitted dielectric relaxation properties for the three DFCLC mixtures. Since  $\Delta\epsilon(\infty)$  is approximately equal to  $\Delta\epsilon(0)$  in these three DFCLC mixtures, the relaxation frequency and crossover frequency are also equal to each other (23). At  $T = 25^\circ\text{C}$ , DFCLC-A shows  $\Delta\epsilon = 3.8$  at the low frequency limit and  $-4.0$  at the high frequency limit. These values are a little smaller than those of the other two mixtures. Large dielectric anisotropy is favourable for achieving fast response time while keeping operating voltage low. Our high birefringence compounds (P1 mixture) exhibit a smaller  $\Delta\epsilon$  than ester-based P2 and P3, as shown in Figure 1; therefore, we need to use a

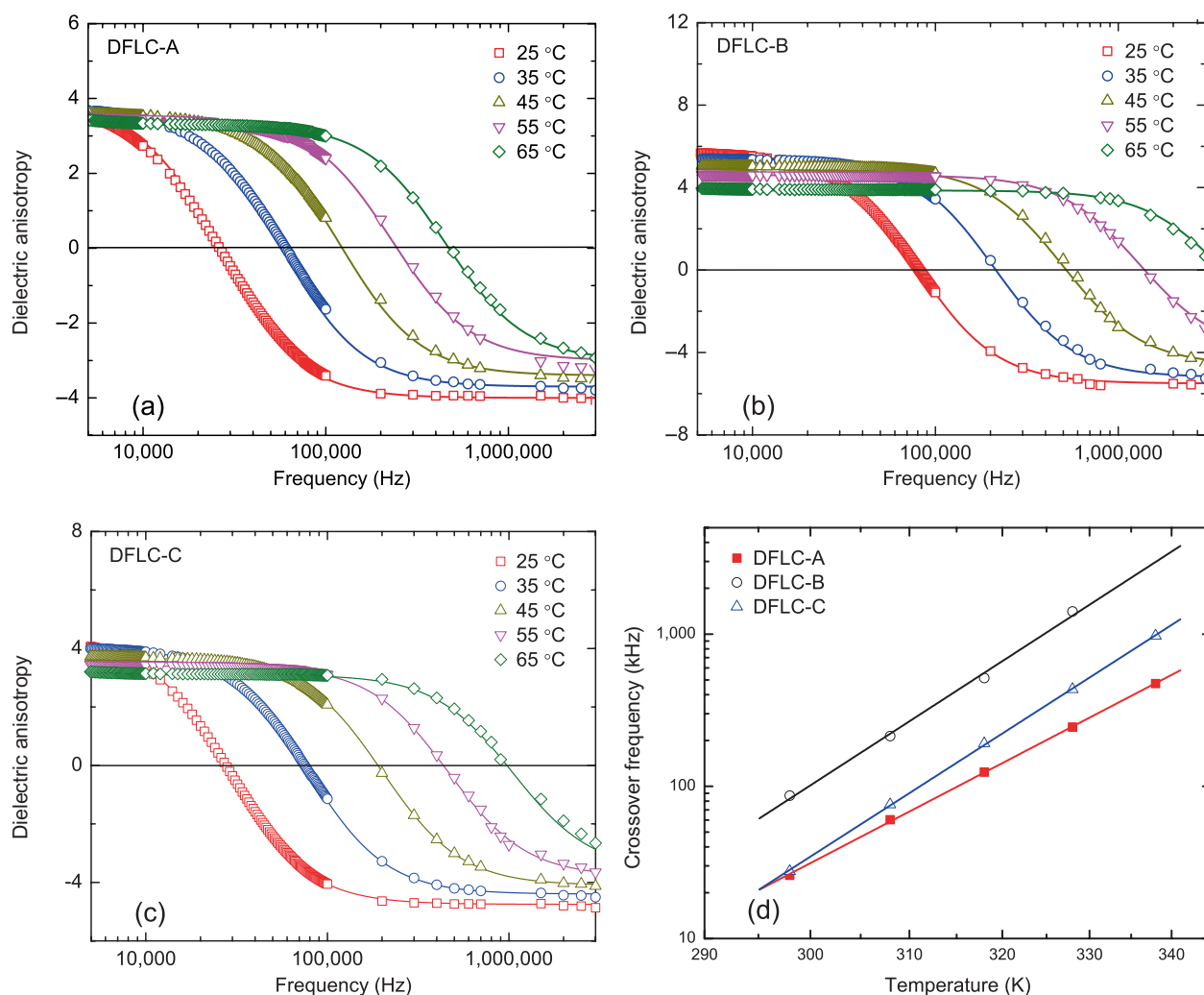


Figure 3. Frequency-dependent dielectric anisotropy of (a) DFCLC-A, (b) DFCLC-B, and (c) DFCLC-C under different temperatures, while (d) shows the temperature-dependent crossover frequency of the three mixtures. Symbols denote experimental results while solid lines correspond to fitting results.

Table 3. Dielectric relaxation properties of DFCL-A, DFCL-B, and DFCL-C at  $T = 25^\circ\text{C}$ .

	$\Delta\epsilon(0)$	$\Delta\epsilon(\infty)$	$f_r$ (kHz)	$E$ (meV)
DFCL-A	3.8	-4.0	26.8	625.7
DFCL-B	5.7	-5.5	80.0	777.0
DFCL-C	4.3	-4.8	28.8	770.1

higher concentration in the final DFCL mixture in order to obtain a symmetric  $|\Delta\epsilon|$ .

The crossover frequencies ( $f_c$ ) for the three DFCL mixtures are plotted against temperature in Figure 3(d). By fitting with Equation (3), we obtain the activation energy for DFCL-A, DFCL-B and DFCL-C, which is 626 meV, 777 meV, and 770 meV, respectively. From Figure 3(d), we found that DFCL-A has the lowest crossover frequency especially for temperatures higher than  $25^\circ\text{C}$  (298 K) as compared with DFCL-B and DFCL-C.

## 5.2 Figure of Merit

It has been demonstrated that the response time of DFCL mixtures is inversely proportional to the Figure of Merit (FoM) defined as (23):

$$FoM_{DFCL} = \frac{(\Delta n)^2 K_{11}}{\gamma_1 V_{th}^2}, \quad (6)$$

where  $V_{th}$  represents the threshold voltage. A higher FoM corresponds to a faster response time from the material point of view. Figures 4(a) and 4(b) show the temperature-dependent birefringence and visco-elastic coefficient of the three DFCL mixtures, respectively, together with the fitting results. With no surprise, DFCL-A exhibits the highest birefringence. Its  $\Delta n = 0.39$  at  $T = 25^\circ\text{C}$  and  $\lambda = 633$  nm is significantly higher than that of DFCL-B (0.24) and DFCL-C (0.26). To our knowledge, this is the highest birefringence ever reported in DFCL mixtures. Our previous record was  $\Delta n \sim 0.29$  (24, 43).

From Figure 4(b), we found the visco-elastic coefficients of the three DFCL mixtures are comparable. At  $T = 25^\circ\text{C}$ , while the visco-elastic coefficient of DFCL-A is slightly lower than that of the other two DFCL mixtures. In comparison to the visco-elastic coefficient of Mixture-A and Mixture-C shown in Figure 2(b), the visco-elastic coefficient of DFCL-A and DFCL-C is almost doubled because of the employed bulky highly conjugated and laterally difluorinated tolane host. On the contrary, DFCL-B exhibits a substantially lower visco-elastic coefficient than Mixture-B because it employs a much smaller concentration (20% vs. 69%)

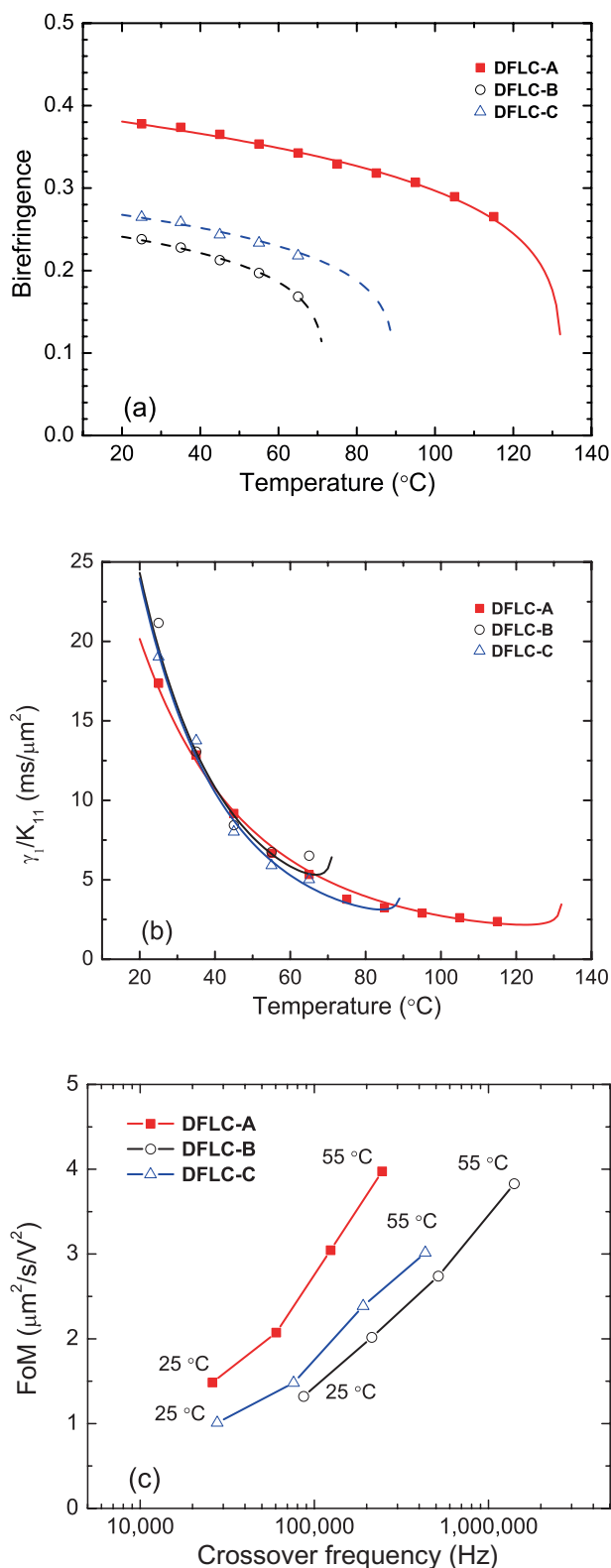


Figure 4. Experimental (symbols) and fitting (curves) results of temperature-dependent (a) birefringence and (b) visco-elastic coefficient of DFCL-A, DFCL-B and DFCL-C, while (c) is a plot of Figure of Merit vs. crossover frequency of these three mixtures at  $25^\circ\text{C}$ ,  $35^\circ\text{C}$ ,  $45^\circ\text{C}$  and  $55^\circ\text{C}$ .



of the viscous CN ester compounds. The calculated FoM for the three DFCL mixtures is plotted against the crossover frequency in Figure 4(c). DFCL-A exhibits the highest FoM and the lowest crossover frequency among the three mixtures compared, which is favourable for practical applications.

## 6. Conclusion

Introducing phenyl tolane positive compounds into DFCL mixtures significantly improves the birefringence. It overcomes the longstanding problem of short conjugation length from the traditional ester positive compounds and thus makes a breakthrough on the birefringence of DFCL materials. We have demonstrated that the DFCL mixture formulated with these new positive compounds shows a birefringence of 0.39 at  $T = 25^\circ\text{C}$  and  $\lambda = 633\text{ nm}$ . Even at IR region ( $\lambda = 1.55\text{ }\mu\text{m}$ ), its birefringence is still as high as 0.33. Also, this DFCL mixture exhibits several other attractive features such as low crossover frequency, low viscoelastic coefficient and high FoM, when compared with the ester-based DFCL mixtures. It is known that the crossover frequency of DFCLs can be greatly reduced by elongating the rigid core of the compounds (24), and we can expect a lower crossover frequency ( $\sim 1\text{ kHz}$ ) if four ring single tolane NCS compounds are employed. Our high  $\Delta n$  DFCL mixtures are useful for reducing the cell gap resulting in a faster response time and lower operating voltage. They are especially attractive in IR applications where UV stability is not a concern.

## Acknowledgements

The authors are indebted to Professors R. Dąbrowski and X. Liang for their technical support and AFOSR for the financial support under Contract No. FA95550-09-1-0170.

## References

- (1) Yang, D.K.; Wu, S.T. *Fundamentals of Liquid Crystal Devices*; Wiley: New York, 2006.
- (2) Golovin, A.B.; Shiyanovskii, S.V.; Lavrentovich, O.D. *Appl. Phys. Lett.* **2003**, *83*, 3864–3866.
- (3) Nie, X.; Wu, T.X.; Lu, Y.Q.; Wu, Y.H.; Liang, X.; Wu, S.T. *Mol. Cryst. Liq. Cryst.* **2006**, *454*, 123–133.
- (4) Lu, Y.Q.; Liang, X.; Wu, Y.H.; Du, F.; Wu, S.T. *Appl. Phys. Lett.* **2004**, *85*, 3354–3356.
- (5) Liang, X.; Lu, Y.Q.; Wu, Y.H.; Du, F.; Wang, H.Y.; Wu, S.T. *Jpn. J. Appl. Phys.* **2005**, *44*, 1292–1295.
- (6) Fan, Y.H.; Ren, H.; Liang, X.; Lin, Y.H.; Wu, S.T. *Appl. Phys. Lett.* **2004**, *85*, 2451–2453.
- (7) Winker, B.; Gu, D.; Wen, B.; Zachery, K.; Mansell, J.; Taber, D.; Sage, K.; Gunning III, W.; Aguilar, M. *Proc. SPIE* **2008**, *6972*, 697209.
- (8) Dayton, D.; Gonglewski, J.; Restaino, S.; Martin, J.; Phillips, J.; Hartman, M.; Browne, S.; Kervin, P.; Snodgrass, J.; Heimann, N.; Shilko, M.; Pohle, R.; Carrion, B.; Smith, C.; Thiel, D. *Opt. Express* **2002**, *10*, 1508–1519.
- (9) Wu, S.T.; Efron, U. *Appl. Phys. Lett.* **1986**, *48*, 624–626.
- (10) Gauza, S.; Zhu, X.; Wiktor, P.; Dabrowski, R.; Wu, S.T., *J. Disp. Technol.* **2007**, *3*, 250–252.
- (11) Jiao, M.; Ge, Z.; Song, Q.; Wu, S.T., *Appl. Phys. Lett.* **2008**, *92*, 061102.
- (12) Wu, S.T.; Efron, U.; Hess, L.D. *Appl. Phys. Lett.* **1984**, *44*, 1033–1035.
- (13) Wu, S.T. *Opt. Eng.* **1987**, *26*, 120–128.
- (14) Wu, S.T.; Wu, C.S. *J. Appl. Phys.* **1989**, *65*, 527–532.
- (15) Wu, S.T. *Appl. Phys. Lett.* **1990**, *57*, 986–988.
- (16) Bücher, H.K.; Klingbiel, R.T.; VanMeter, J.P. *Appl. Phys. Lett.* **1974**, *25*, 186–188.
- (17) Schadt, M. *Mol. Cryst. Liq. Cryst.* **1981**, *66*, 319–336.
- (18) Schadt, M. *Annu. Rev. Mater. Sci.* **1997**, *27*, 305–379.
- (19) Dabrowski, R.; Kula, P.; Gauza, S.; Dziaduszek, J.; Urban, S.; Wu, S.T. *Proc. IDRC* **2008**, 35–38.
- (20) Wu, S.T.; Hsu, C.S. Chen, J.M. *Mol. Cryst. Liq. Cryst.* **1997**, *304*, 441–445.
- (21) Wen, C.H.; Gauza, S.; Li, J.; Wang, H.Y.; Wu, S.T. *Liq. Cryst.* **2005**, *32*, 643–649.
- (22) Xianyu, H.; Gauza, S.; Song, Q.; Wu, S.T. *Liq. Cryst.* **2007**, *34*, 1473–1478.
- (23) Xianyu, H.; Wu, S.T.; Lin, C.L. *Liq. Cryst.* **2009**, *36*, 717–726.
- (24) Xianyu, H.; Zhao, Y.; Gauza, S.; Liang, X.; Wu, S.T. *Liq. Cryst.* **2008**, *35*, 1129–1135.
- (25) Ziobro, D.; Kula, P.; Dziaduszek, J.; Filipowicz, M.; Dąbrowski, R.; Parka, J.; Czub, J.; Urban, S.; Wu, S.T. *Opto-electron. Rev.* **2009**, *17*, 16–19.
- (26) Ziobro, D.; Dziaduszek, J.; Filipowicz, M.; Dąbrowski, R.; Czub, J.; Urban, S. *Mol. Cryst. Liq. Cryst.* **2009**, *502*, 258–271.
- (27) Wu, S.T.; Ramos, E.; Finkeneller U. *J. Appl. Phys.* **1990**, *68*, 78–85.
- (28) Wu, S.T.; Cox, R.J. *J. Appl. Phys.* **1988**, *64*, 821–826.
- (29) Wu, S.T.; Hsu, C.S.; Shyu, K.F. *Appl. Phys. Lett.* **1999**, *74*, 344–346.
- (30) Sekine, C.; Fujisawa, K.; Iwakura, K.; Minai, M. *Mol. Cryst. Liq. Cryst.* **2001**, *364*, 711–718.
- (31) Gauza, S.; Wang, H.; Wen, C.H.; Wu, S.T.; Seed, A.J.; Dąbrowski, R. *Jpn. J. Appl. Phys.* **2003**, *42*, 3463–3466.
- (32) Gauza, S.; Wen, C.H.; Wu, S.T.; Janarthanan, N.; Hsu, C.S. *Jpn. J. Appl. Phys.* **2004**, *43*, 7634–7638.
- (33) Catanescu, O.; Chien, L.C. *Liq. Cryst.* **2006**, *33*, 115–120.
- (34) Seed, A.J.; Toyne, K.J.; Goodby, J.W.; Hird, M. *J. Mater. Chem.* **2000**, *10*, 2069–2080.
- (35) Gauza, S.; Parish, A.; Wu, S.T.; Spadło, A.; Dąbrowski, R. *Mol. Cryst. Liq. Cryst.* **2008**, *489*, 135–147.
- (36) Gauza, S.; Parish, A.; Wu, S.T.; Spadło, A.; Dąbrowski, R. *Liq. Cryst.* **2008**, *35*, 483–488.
- (37) Wu, S.T.; Wu, C.S. *Phys. Rev. A* **1990**, *42*, 2219–2227.
- (38) Wu, S.T.; Efron, U.; Hess, L.D. *Appl. Opt.* **1984**, *23*, 3911–3915.
- (39) Schadt, M. *Mol. Cryst. Liq. Cryst.* **1982**, *89*, 77–92.
- (40) Haller, I. *Prog. Solid State Chem.* **1975**, *10*, 103–110.
- (41) Wu, S.T. *Phys. Rev. A* **1986**, *33*, 1270–1274.
- (42) Wu, S.T.; Lackner, A.M.; Efron, U. *Appl. Opt.* **1987**, *26*, 3441–3445.
- (43) Wen, C.H.; Wu, S.T. *Appl. Phys. Lett.* **2005**, *86*, 231104.